Eur. Phys. J. B **75**, 49–56 (2010)
DOI: 10.1140/epjb/e2010-00054-1

THE EUROPEAN PHYSICAL JOURNAL B

Regular Article

A spin-selective approach for surface states at Co nanoislands

B.W. Heinrich[1], C. Iacovita[1], M.V. Rastei[1], L. Limot[1], P.A. Ignatiev[2], V.S. Stepanyuk[2], and J.P. Bucher[1,a]

[1] Institut de Physique et Chimie des Matériaux de Strasbourg, UMR 7504, Université de Strasbourg, 67034 Strasbourg, France
[2] Max-Plank-Institute für Mikrostrukturphysik, Weinberg 2, 06122 Halle, Germany

Received 5 November 2009 / Received in final form 11 January 2010
Published online 16 February 2010 –

Abstract. During recent years the surface electronic states of cobalt nanoislands grown on Cu(111) and Au(111) have been extensively studied and still yield fascinating results. Among magnetic surfaces, cobalt islands are particularly appealing because of their spin-polarized electronic states near the Fermi energy, involving localized d states of minority character, as well as free-like $s-p$ states of majority character. We show here that these states are a sensitive probe to minute changes of structural details such as strain and stacking, and therefore constitute an ideal playground to study the interplay between structural and spin-related properties. Due to their size, cobalt islands on Cu(111) offer the additional opportunity to host single-magnetic adsorbates suitable for spin-polarized scanning tunneling microscopy and spectroscopy (SP-STM and SP-STS). We establish here that, in an energy interval just below the Fermi level, the spin-polarization of a transition-metal atom is governed by surface-induced states opposite in sign compared to the island, while the spin-polarization of Co-Phthalocyanine molecules is governed by molecular states. This opens up interesting perspectives for controlling and engineering spin-polarized phenomena at the nanoscale.

1 Introduction

One of the major challenges nowadays in the development of spintronic devices is to understand the spin transport through single atoms and molecules. This task is of great complexity essentially because the electronic states depend on many structural and environmental parameters, which are usually difficult to unveil. One way to study the spin-transport properties consists in bringing two magnetic electrodes into contact with each other or with a single molecule [1–4]. A strong point of this technique is the possibility of implementing a third electrode, isolated from the first two, in order to apply a gate bias. A complementary approach to study spin-transport at the nanoscale is spin-polarized (SP) scanning tunneling microscopy and spectroscopy (STM and STS). These techniques can visualize the spin state of an atom [5,6] or a molecule [7], so to carefully correlate changes in the spin-polarized states with changes in the adsorbate-metal interface. In this way an absolute control is achieved over structural details, which are known to play an important role in contact measurements.

In this paper, we show that cobalt islands grown on Cu(111) and Au(111) are model spin-polarized systems. By combining SP-STM and STM studies with ab initio calculations, we establish the spin-polarized nature of their surface states and how they are affected by structural details such as strain and stacking. Due to their large surface area, cobalt islands on Cu(111) offer the additional opportunity to host single-magnetic adsorbates. The spin of these adsorbates couples to the out-of-plane magnetization of the islands, so that a spin-contrast among adsorbates is achieved even in the absence of a magnetic field. We show in particular that atoms and molecules locally modify the spin-polarization of the island: in an energy interval just below the Fermi level, atoms have a spin-polarization dominated by surface-induced states and opposite in sign compared to the pristine island, while Co-Phthalocyanine (CoPc) molecules have a spin-polarization dominated by molecular states. The combination of an adsorbate and a magnetic surface therefore provides a route for controlling spin-polarized phenomena at the nanoscale.

2 Experimental setup

All the measurements presented were performed in a STM operating below 10^{-10} mbar at temperatures of 2.8 K and 4.6 K. After cleaning the Au(111) and Cu(111) single crystal by repeated cycles of Ar^+ sputtering and annealing to 500 °C, the surface was cooled to room temperature. Cobalt was subsequently deposited onto these surfaces by e-beam evaporation at submonolayer coverage to form self-assembled nanoislands. A variety of etched W and Ni

[a] e-mail: bucher@ipcms.u-strasbg.fr

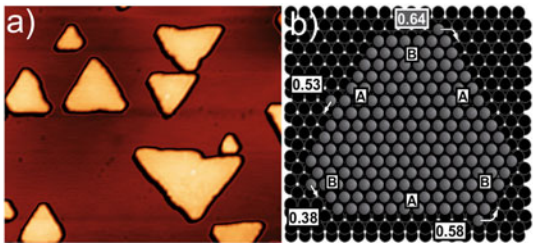

Fig. 1. (Color online) (a) STM image of Co nanoislands grown at room temperature on a Cu(111) surface (90×80 nm^2, 0.10 nA, -0.26 V). (b) Schematic representation of a single-layer island and of the adatom diffusion along the island edges and corners (Cu: black, Co: grey). The barrier height (in eV) is indicated for distinct positions of the adatoms.

tips were employed. After a sputter/anneal cycle, the tips were treated by soft indentations into the surface, until tip-structure artifacts were minimized in the differential conductance (dI/dV) spectra over the voltage range of interest. The dI/dV versus sample bias (V) was recorded by superimposing a sinusoidal modulation to the junction bias (amplitude: 5−10 mV rms, frequency: 3−7 kHz), and detecting the first-harmonic of the current through a lock-in amplifier.

Spin-polarized measurements were performed with Co−Coated Ni tips since we found that they posses an out-of-plane component of the magnetization parallel to the island magnetization. The spin-dependent contribution to the differential conductance varies in fact with $\cos\theta$, where θ is the angle between the magnetization of the tip and of the sample [8].

Single atoms and molecules were deposited on the cobalt nanoislands following distinct procedures. Ni, Co, and Cu atoms were deposited onto the substrate by a controlled transfer of the tip-apex atom [9], so that isolated atoms residing in the island center could be obtained (see Fig. 9a). The coating material for the tip apex was therefore chosen accordingly to the desired atom. The CoPc molecules were sublimated onto the sample by heating to at least 400 °C a crucible containing a 99.5% pure CoPc powder. Typical island coverage was roughly 10 molecules for an area of (10 nm)^2.

3 A model magnetic electrode

3.1 Growth and stacking

At room temperature the deposition of cobalt onto Cu(111) leads, at a submonolayer coverage, to the formation of compact triangular structures as shown in Figure 1a [10–15]. These islands are two-atomic-layers high and have lateral sizes up to 30 nm. Smaller island sizes on the order of 5 nm can be obtained by using other noble metal surfaces like Au(111) [16–21]. Most importantly, these islands possess, at our working temperature, a magnetization perpendicular to the surface with a "up" or "down" orientation.

The shape of the nanoislands is determined by a variety of parameters. An important one is the activation barrier for the diffusion of the adsorbed atoms along a nucleated-island edge and corner, as schematically shown in Figure 1b. Additional details about the calculation of the activation barriers and how these define the shape of the nanoislands can be found in reference [12]. The symmetry of the (111) surface determines two types of island edges, namely one with a {100}-orientation, labeled A in Figure 1b, and another one with a {111}-orientation, labeled B. The Co adatoms can easily diffuse along both edges and also jump from A to B. The reverse hopping is less probable because of the higher activation barrier. This suggests that, at least in the initial stage of growth when single atomic layers can be energetically stable, the {100} edges grow at the expense of the {111} edges favoring a triangular shape. The islands grow two atomic-layer thick because: (i) the diffusion on the first layer is favored compared to the downward hopping onto the surface; (ii) the downward motion from the third layer is favored compared to the upward motion. Figure 1a also shows that the nanoislands are oriented in two opposite directions. This follows from the two possible nucleation sites of Co on the surface, either *hcp* or *fcc*, leading respectively to islands with a faulted and unfaulted stacking.

3.2 Spin-polarized surface states

At the surface of crystals the electronic states can substantially differ with respect to the bulk states because the translational symmetry of the crystal is broken. A well-known example illustrating these differences is the existence of a special class of electronic states bound to the crystal surface [22,23]. At metallic substrates such surface states appear in the projected energy gaps of the bulk band structure, for instance, in the inverted $\bar{L}$-gaps of {111}-surfaces of noble metals. The existence of these dispersive surface states were predicted by Shockley [23], and subsequently observed by angle-resolved photoemission spectroscopy [24]. On nanostructures, Shockley surface states can be evidenced and studied by means of low-temperature STM and STS [25,26]. In addition to these surface states, transition metals can also have d-states near the Fermi level. Identifying the nature of these surface states may therefore prove to be quite challenging in a magnetic nanostructure without a solid theoretical support.

This scenario is indeed encountered in cobalt nanoislands, as they host $s-p$ surface states [13,28], as well as localized d-states near E_F [13–15]. Figure 2 presents typical STS spectra measured in the center of faulted and unfaulted nanoislands grown on Cu(111) and on Au(111). On both substrates the nanoislands have three distinct peaks, two below the Fermi level and one above. On Cu(111) the occupied states on unfaulted islands have a dominant peak at -0.31 V. The same peak falls at a higher energy of -0.28 V on faulted islands. At lower energies, a second peak is present which also shifts with stacking order. The unoccupied states have a peak at 0.30 V which

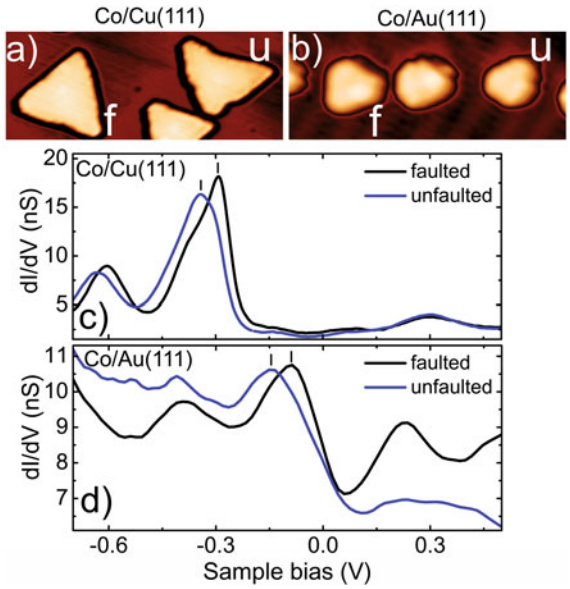

Fig. 2. (Color online) STM images of Co nanoislands on (a) Cu(111) (60×25 nm^2, 0.10 nA, -0.26 V), and (b) Au(111) (24×10 nm^2, 0.50 nA, 0.10 V) (b). Triangular islands with opposite orientation, i.e. different stacked islands, are labeled f (faulted) and u (unfaulted). Typical dI/dV spectra measured over Co nanoislands on (c) Cu(111) (feedback open at 1.50 nA, 0.60 V), and (d) Au(111) (feedback open at 0.53 nA, 0.10 V). The Fermi level corresponds to a zero sample bias. The short lines indicate the main d peak of the islands.

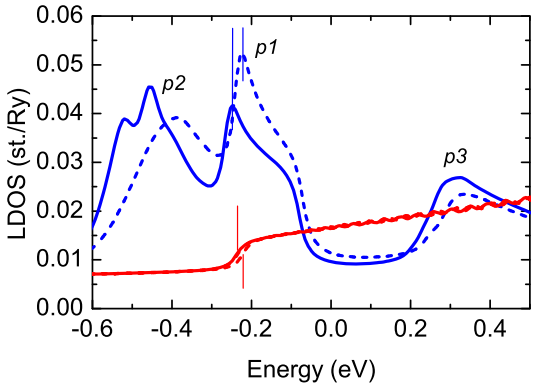

Fig. 3. (Color online) Spin-polarized LDOS calculated by means of the KKR Green's function method above a unfaulted (solid lines) and faulted (dashed lines) infinite Co-bilayer on Cu(111). Minority spin states are in blue, whereas majority spin states are in red.

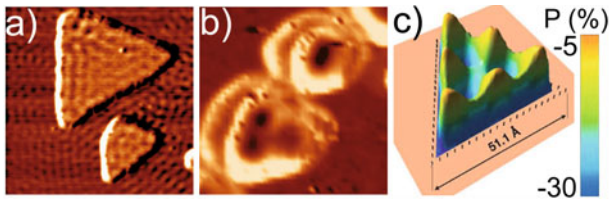

Fig. 4. (Color online) dI/dV maps of Co nanoislands on (a) Cu(111) at 0.10 V (30×30 nm^2, feedback open at 0.50 nA, 0.10 V), and (b) Au(111) at 0.70 V (12×12 nm^2, feedback open at 0.75 nA, 0.12 V). (c) Calculated spin polarization on a Co nanoisland on Cu(111) at energy of 0.5 eV. Figure 4c is adapted from reference [27].

is independent of stacking order. On Au(111) the spectra are quite similar, however the peaks for the occupied states are significantly higher in energy. The unfaulted islands exhibit a dominant peak at -0.15 V, whereas for the faulted ones the peak appears at about -0.09 V. Additional peaks appear at higher and lower energies compared to Cu(111), although they present a distribution in amplitude and in energy position due to the reduced size of the islands.

To reveal the origin of these surface states, theoretical calculations were performed by means of the Korringa-Kohn-Rostoker (KKR) Green's function method based on density functional theory [29–31]. The surface states above the center of each island were estimated by performing calculations for an infinite cobalt bilayer. These studies show that in this energy range, electronic states of different orbital and spin character coexist. In Figure 3 we present the computed local density of states (LDOS) for the Co on Cu(111) system [15]. As shown, minority states present localized peaks at specific energies that fit well with the experimental data. Moreover by changing the stacking order, the calculations are able to reproduce the peak shift of the faulted and unfaulted islands. A similar result is also found for Co on Au(111) [20]. A detailed inspection of the spectral density maps (imaginary part of the momentum-resolved energy-dependent Green's function) indicates that the peaks originate from d-bands of Co at distinct energies in the reciprocal space. The peaks below the Fermi energy result from $d_{3z^2-r^2}$ orbitals. In particular, we assign the main peak in the STS spectra to a hybridization of $s-p$ states with the minority $d_{3z^2-r^2}$ states situated in the bulk band gap. The peak at lower energy is traced back to a resonant overlapping of Cu(111) bulk states with the Co minority $d_{3z^2-r^2}$ states. Finally, the peak above the Fermi level originates from the unoccupied minority d band of the Co islands, which is less sensitive to the stacking order because of its non-dispersive character.

Figure 3 shows that the majority states are dominated by dispersive states with a step-like onset predicted near -0.23 eV. This onset should also be measured experimentally by STS but is buried below the dominant d-like peak. However, due to the dispersive nature of these states it is possible to observe their confinement in the island at various energies. Experimentally, this is done by acquiring dI/dV spectral maps at fixed sample biases. As an example, Figures 4 shows two dI/dV maps recorded over Co nanoislands on Cu(111) (Fig. 4a) and Au(111) (Fig. 4b). Standing-wave patterns can be visualized and exploited to estimate the dispersion of theses states [13,14], following a well known procedure experimented on Shockley surface states [25,26]. The bottom edge of the band is estimated at -0.20 V, or lower, in fair agreement with predictions. Due to the smaller size of the Co nanoislands on Au(111) (Fig. 4b), the spatial oscillations of the dI/dV

Table 1. Sample bias (U) corresponding to the dominant peak position of unfaulted Co nanoislands as a function of the macroscopic mismatch with the underlying substrate (M).

	Au(111)	Pt(111)	Cu(111)	Co(film)
M (%)	13	9	2	0
U (V)	−0.15	−0.23 Ref. [33]	−0.31	−0.43 Ref. [34]

signal over these structures are even more pronounced and located at higher energies. We find a bottom edge of the band at about −0.10 eV, in good agreement with theory (not shown here). Recently, the bottom edge of the band was estimated at 0.10 V for Co islands grown on Au thin films [21].

An important consequence of the confinement of the majority $s-p$ surface states is that a spatial change of the spin-polarization is expected over the nanoislands. The spatially-resolved spin polarization calculated as

$$P(\mathbf{r}, E) = [n_\uparrow(\mathbf{r}, E) - n_\downarrow(\mathbf{r}, E)] \,/\, [n_\uparrow(\mathbf{r}, E) + n_\downarrow(\mathbf{r}, E)] \quad (1)$$

shows in fact significant oscillations over a Co nanoisland as presented in Figure 4c. This is due to the fact that the density $n_\downarrow(\mathbf{r}, E)$ of minority states can be assumed constant in the inner part of the island, while the density $n_\uparrow(\mathbf{r}, E)$ of the majority states exhibits oscillations. Since the size of the nanoislands affects the amplitude of these oscillations, a size-dependent spin-polarization is also predicted for these islands [27].

3.3 How strain changes the surface states

The size of the island can also impact the spin-polarization via the strain existing in the island. Generally speaking, nanostructures epitaxially grown on a substrate tend to adopt the lattice parameter of the underlying surface. As a consequence the bond lengths between the metal atoms in the supported nanostructures differ from those in the parent metals, resulting in strain. A theoretical study on homoepitaxial double layer Cu islands on Cu(111) has shown that the strain produces an inhomogeneous distribution of bond lengths over the nanoisland, the average bond length varying with island size [32]. As was pointed out quite early by Friedel (1969) [35], surface states are a sensitive probe for variations of the atomic structure at the nanoscale and, in this regard, strain is expected to play an important role [15,36–38].

To attest the sensitiveness of surface states to atomic bond lengths, we may turn back to the surface states of the Co nanoislands on Cu(111) and on Au(111) presented in Figure 2. An important difference between the Cu(111) and Au(111) surfaces is the interatomic bond length, respectively 0.256 nm and 0.289 nm, so that the Co nanoislands on Au(111) are submitted to a larger tensile stress compared to those on Cu(111). Table 1 presents the energetic position of the main peak as a function of the macroscopic mismatch for Co on Au, Cu and Pt(111) (from Ref. [33]). We have included also data for a Co thin film [34]. The macroscopic mismatch is defined as

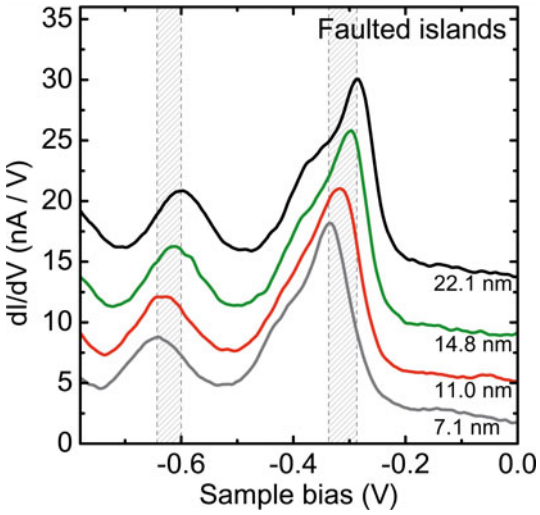

Fig. 5. (Color online) (a) dI/dV spectra acquired in the center of faulted Co nanoislands on Cu(111) (feedback loop opened at 1.5 nA, 0.6 V). The hatched areas indicate the interval over which the shift occurs. The island-edge length is indicated for each spectrum.

$M = (d_{\mathrm{Sub}} - d_{\mathrm{Co}})/d_{\mathrm{Sub}}$, where d_{Sub} and d_{Co} are the bulk bond length of the substrate and of Co, respectively. As shown the smaller the bond length of the substrate, the lower the energy of the d-like peak. In other words, the position of this peak is sensitive to the in-plane Co−Co bond length. As a result, the lateral compression or expansion of the Co nanoislands by the substrate underneath is found to be the driving force for the shift of this peak.

Direct evidence of strain effects in Co islands is gathered by performing STS over islands of different size. This was done over more than 200 faulted and unfaulted islands of Cu(111) [15]. This is difficult to carry out on Au(111), because the size distribution of the islands is ≈2 nm and edge effects (see below) are important given their reduced size. Unfaulted islands with an edge length ranging from 4.8 to 31.9 nm, and faulted islands with an edge length ranging from 6.7 to 32.9 nm were investigated on Cu(111). Figure 5 presents a set of dI/dV spectra acquired on faulted Co nanoislands of different sizes. Size-dependent changes in spectra are marked by hatched areas. As shown, the peaks below the Fermi level shift downward in energy when the island size decreases from 22.1 to 7.1 nm, with no appreciable changes in the shape of the spectra (similar results were also obtained for the unfaulted islands). The quantitative evaluation of the data reveals that the shifts are significant only for nanoislands with a size below 12 nm. Beside this size-dependent shift, strain also plays a role within the island. When dI/dV spectra are recorded at different locations of the islands, for example by moving the tip from a corner to the opposite edge, the d-peak shows an additional displacement, shifting to lower energy when approaching the corner or the edge [15]. These changes evidence a bond length variation within the nanoisland, with the exception of an area of a few nanometers in the center of the island (see also Fig. 6a).

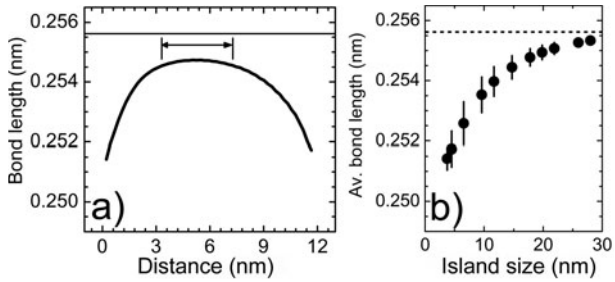

Fig. 6. (a) Computed variation of the in-plane bond length in the top Co layer of a nanoisland with an edge length equal to 15 nm. The arrow indicates the zone where the bond lengths are nearly constant. (b) Average bond length of the center part of the nanoislands as a function of nanoisland size. The horizontal lines show the ideal bulk Cu bond length.

A number of theoretical calculations were performed in order to model the size- and position-dependent shifts of the occupied surface states. A first set includes the calculation of the relaxed atomic configuration inside the nanoislands. This was performed by molecular dynamics [32,37,39], i.e. by solving the equations of motion for all the atoms in the system. Atomic interactions were modeled in the second moment of the tight-binding approximation. Various Co nanoislands with different sizes were studied. The results confirm that both in-plane and out-of-plane bond lengths depend on the nanoisland size and vary across the nanoisland. The distribution of the in-plane bond lengths of the topmost Co layer over a 15 nm island is presented as an example in Figure 6a. The bond lengths are inhomogeneous over the island. At the edges and corners the atoms relax toward the center of the nanoisland and adopt other equilibrium positions with shorter bond lengths with respect to Co atoms in the center of the nanoisland. The inner region around the gravity center of each nanoisland presents nearly homogeneous bond lengths and an average in-plane bond length can be used to describe this region. This zone is schematically represented by an arrow in Figure 6a. Figure 6b shows the average bond lengths of this central region for different nanoisland sizes. As shown, the average bond length increases when the nanoisland size increases. An asymptotic behavior sets in when the bond length approaches the ideal bond length of bulk Cu, which confirms the STS findings of a negligible shift for nanoislands larger than 12 nm.

4 Spin structure of nanoscale objects

4.1 Cobalt nanoislands

Nowadays the only techniques that allow to inject SP tunneling electrons with atomic-scale resolution are SP-STM and SP-STS [40,41]. In particular, they are well suited for identifying the SP nature of the island surface states. STS on the islands [13], motivated a series of SP-STS studies on both Cu [5,7,14,28,42], and Au systems [43,44], confirming most of the theoretical predictions mentioned above.

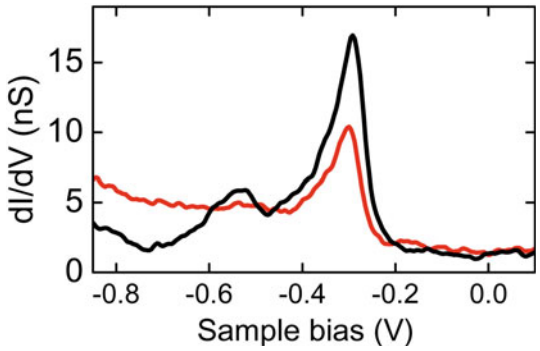

Fig. 7. (Color online) Spin-polarized dI/dV spectra of two Co nanoislands with opposite magnetization on Cu(111) (feedback open at 0.50 nA, 0.60 V).

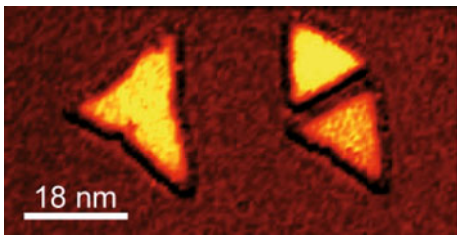

Fig. 8. (Color online) Spin-polarized dI/dV maps of three Co nanoislands at -0.28 V (size 76×36 nm^2, feedback open at 0.50 nA, 0.60 V). The two unfaulted islands (those pointing left) have different intensities, and therefore have opposite magnetizations and spin-polarizations.

All these experiments indicate that the d-peaks detected below the Fermi level are SP electronic states. Figure 7 presents two SP-STS spectra over two cobalt nanoislands of opposite magnetization. The main peak in the two spectra falls at the same position, but differs in amplitude. While the differential conductivity at the peak position amounts to only 11 nS for one nanoisland, it is enhanced by 50% for the second. The relative intensities of spectra can invert at some biases, revealing a complex SP tunneling transport between the islands and the tip. Given this bias dependence we cannot identify the orientation of the magnetization, neither in the nanoislands nor in the tip. However, we may safely conclude that the analyzed nanoislands have an opposite magnetization (or opposite spin polarization), in agreement with measurements under external magnetic fields [14,42].

The differential conductivity of the nanoislands can be mapped at a bias where a SP signal is detected in the spectra. The most advantageous situation is to fix the bias where the ratio between the two dI/dV amplitudes acquired on islands of opposite magnetization is high, for example close to the d-like peak. The resulting SP dI/dV map is presented in Figure 8 and shows a clear spin contrast among the islands. However care must be taken when comparing these contrasts [14]. From Figures 2c and 5 we know in fact that the stacking and size of the islands shift the main peak. This shift then translates into a contrast in the dI/dV maps, thereby "polluting" the spin contrast. This is why it is essential to compare the contrast between

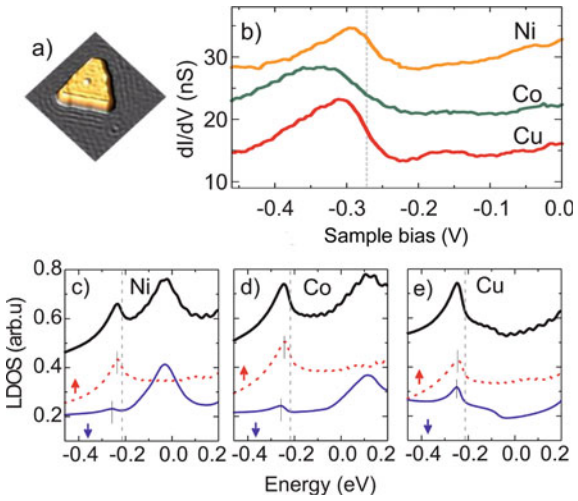

Fig. 9. (Color online) (a) Faulted cobalt island with a Cu atom in its center (24×24 nm^2, 0.3 nA, 0.03 V). (b) dI/dV spectra over Ni, Co, and Cu atoms deposited near the center of a Co nanoisland (feedback open at 0.4 nA, 0.03 V). The Ni and Co spectrum is displaced vertically by 14 and 7 nS, respectively. (c−e) Calculated spin-polarized LDOS above Ni, Co and Cu atoms on a faulted cobalt bilayer. The dashed-red lines represent the majority states, while the solid-blue ones the minority states. The total LDOS is plotted by thick-black lines. The dashed vertical lines indicate the majority $s-p$ surface-state onset.

islands of same stacking and of same size (or larger than 12 nm), where the size related shift becomes negligible.

4.2 Single-magnetic atoms and molecules

As was highlighted in the previous sections, cobalt islands on Cu(111) constitute a well-known spin-polarized system. Additionally, due to their large surface area and flat structure they are well suited for hosting single atoms and molecules. With a near-field technique it is therefore possible to compare on a local stand the spin-polarization of an adsorbate and of a clean magnetic island. Information may be gathered on how minute structural details influence the spin-polarization. This has recently motivated STS [45,46], and SP-STS [5,7], studies of single adsorbates on these islands.

Atoms. SP-STS of individual Fe and Cr atoms on cobalt islands of Cu(111) was performed by means of a Cr-covered tungsten tip [5]. From the dI/dV spectra it was found that the two atoms have different spin-polarizations in a bias-range close to the Fermi level. Although theoretical calculations reveal a ferromagnetic coupling between the Fe atoms and the island and an antiferromagnetic coupling for the Cr atoms, the spin-structure evidenced for the two atoms remained unclear. This motivated a new combined experimental and theoretical study on single Ni, Co and Cu atoms. STS was performed over the three atoms, which were transferred from the tip apex to the center of the island through a controlled tip-surface contact (Fig. 9a), see Section 2. The dI/dV spectra are presented in Figure 9b. Surprisingly, the spectra are very similar, indicating a common origin of the observed feature around −0.30 V.

Calculations performed within density functional theory implemented in the multiple-scattering KKR Green's function method [45], indicate that electronic states above the atoms are spin-polarized, the atom-island coupling being ferromagnetic. The calculated magnetic moments are 2.00 μ_B (Co), 0.74 μ_B (Ni) and 0.03 μ_B (Cu). Figures 9c−9e show the SP local density of states at roughly 0.42 nm above the investigated atom. Several conclusions may be drawn from Figures 9c−9e. The majority LDOS (dashed-red lines in Figs. 9c−9e) is found to dominate the minority LDOS (solid-blue lines) in this energy range. In other words, the spin-polarization defined in equation (1) is opposite in sign over the adatoms compared to the clean island. The common resonance detected in STS (Fig. 9b) can be assigned to the localization of the dispersive $s-p$ surface states at the adatom site, which is a well known phenomenon also encountered on non-magnetic substrates [47–51]. The localization occurs at an energy close to the onset of the $s-p$ states (dashed line in Figs. 9c−9e) and is responsible for an enhancement of the spin-polarization in this energy range since the localization is of majority character. Some atoms also possess contributions from atomic d-resonances. These resonances increase the minority channel over finite energy ranges: at the Fermi level for the Ni atom (Fig. 9c) and around 0.10 V for the Co atom (Fig. 9d). If these resonances are sufficiently strong, they may invert the sign of the spin-polarization over the atoms. This occurs, for example, for the Cr atom [45].

These findings have also important implications for SP-STM. A surface in fact mimics a tip apex with a poor spatial resolution (also known as a blunt tip), while an individual adatom approximates well the monoatomic tip apex used in SP-STM [52,53]. As demonstrated above, the spin states of this atomic protrusion arise from atomic-like and surface-induced states. Contrary to the first, the second contribution is predicted to favor in vacuum a change in sign of the spin polarization, indicating that minute changes in the tip-apex structure can yield opposite spin-polarizations. We expect this result to be robust on tip-apex contaminations, for example if the apex atom is a weakly-magnetic Cu atom (Fig. 9e), in agreement with recent findings [53].

Molecules. SP-STM and SP-STS studies can also be extended to single molecules. This is done by depositing single CoPc molecules on the cobalt islands. Figure 10a shows the typical adsorption of CoPc on the Co/Cu(111) system. Below 0.1 monolayers CoPc adsorbs preferentially on cobalt, either on top of the nanoislands or along the edges. On the islands, CoPc exhibits a four-lobe pattern 1.4 nm wide consistent with the ideal structure of the molecule (Fig. 10b). Prior to the SP-STS measurements we performed extensive STS measurements on molecules adsorbed on a large number of islands and all the spectra were identical, indicating that the molecular adsorption is the same on the islands of same stacking. Spin-polarized

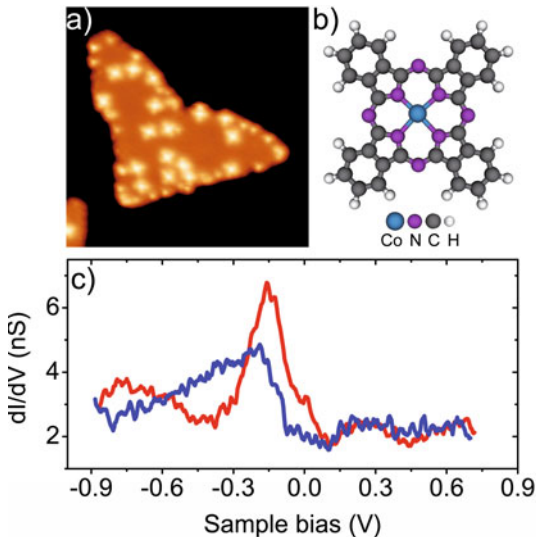

Fig. 10. (Color online) (a) STM image of CoPc molecules deposited on a Co nanoisland grown on Cu(111) (25×25 nm^2, 0.1 V, 1.0 nA). (b) The model structure of the CoPc molecule (c) dI/dV spectra acquired over the center of single CoPc molecules adsorbed on Co nanoislands of opposite magnetization (feedback open at 0.6 V, 0.5 nA).

dI/dV spectra are presented in Figure 10c for molecules residing on islands of opposite magnetization. The dI/dV, which were acquired over the cobalt atom of CoPc, present a peak-like feature at -0.15 V that differs in amplitude depending on the "up" or "down" orientation of the island magnetization. As in the case of the cobalt islands (Fig. 7), this result indicates that the molecules have SP states in this bias range. While this spin-polarized feature is fairly reproducible, the spectra at lower biases are tip dependent. This probably arises from different atomic configurations of the tip apex (see Sect. 4.2). Nevertheless, these spectra show that CoPc molecules residing on islands of opposite magnetization have an opposite spin-polarization, which can then be visualized through dI/dV maps [7]. These maps show, in particular, that the SP signal is located above the Co atom of CoPc.

First-principles calculations based on density functional theory by means of the PWscf package were carried out to gain insight into the spin polarization of CoPc observed by SP-STM. A detailed presentation of the calculations can be found elsewhere [7]. In the lowest energy configuration, the Co atom of the molecule is found to adopt a bridge position with respect to the substrate atoms. This is in part due to the N atoms, which participate along with the rest of the benzopyrrole rings to the covalent bond with the nanoisland. Theoretical calculations show that the SP-STS signal is carried by minority d_{xz}, d_{yz} and d_{z^2} states of Co. The magnetic coupling between the molecule and the Co island is found to be ferromagnetic and arises from a direct $\mathrm{Co}-\mathrm{Co}_{\mathrm{surface}}$ exchange interaction, as well as from an indirect $\mathrm{Co}-\mathrm{N}-\mathrm{Co}_{\mathrm{surface}}$ superexchange interaction. The ligands of the molecule therefore actively influence the SP properties of the molecule through the adsorption of CoPc on the island, and through the magnetic coupling. This opens up the interesting perspective of optimizing the spin-polarization by a careful choice of the ligands that link the molecule to the surface.

5 Conclusions

To summarize, we presented the surface electronic states of cobalt nanoislands grown on Cu(111) and Au(111). These spin-polarized states involve d-like localized states of minority character, as well as free-like $s-p$ states of majority character near the Fermi energy, which were shown to be sensitive to structural details such as strain and stacking. Cobalt islands on Cu(111) were also used as a magnetic substrate to support single-magnetic adsorbates accessible by SP-STM and SP-STS. In an energy interval just below the Fermi level, the spin-polarization of these adsorbates was shown to be governed by surface-induced states and by adsorbate-related states. Both contributions are present in the atoms, the surface-induced states favoring a change in sign of the spin-polarization with respect to the island. The spin-polarization of the molecules, on the contrary, is governed by molecular states, which for CoPc correspond to the minority d-states of the central Co atom. The combination of a carefully chosen adsorbate with a magnetic surface constitutes a spin-selective approach for SP engineering.

This work was supported by the European Union Network of Excellence MAGMANet (FP6-515767-2) and the Agence Nationale de la Recherche (ANR-07-BLAN-0139). Financial support by the DFG through the Schwerpunktprogramm 1153 is gratefully acknowledged.

References

1. B. Doudin, M. Viret, J. Phys.: Condens. Matter. **20**, 083201 (2008)
2. M.R. Sullivan, D.A. Boehm, D.A. Ateya, S.Z. Hua, H.D. Chopra, Phys. Rev. B **71**, 024412 (2005)
3. M. Viret, M. Gabureac, F. Ott, C. Fermon, C. Barreteau, G. Autes, R. Guirado-Lopez, Eur. Phys. J. B **51**, 1 (2006)
4. K. Tsukagoshi, B.W. Alphenaar, H. Ago, Nature **401**, 572 (1999)
5. Y. Yayon, V.W. Brar, L. Senapati, S.C. Erwin, M.F. Crommie, Phys. Rev. Lett. **99**, 067202 (2007)
6. F. Meier, L. Zhou, J. Wiebe, R. Wiesendanger, Science **320**, 82 (2008)
7. C. Iacovita, M.V. Rastei, B.W. Heinrich, T. Brumme, J. Kortus, L. Limot, J.P. Bucher, Phys. Rev. Lett. **101**, 116602 (2008)
8. D. Wortmann, S. Heinze, Ph. Kurz, G. Bihlmayer, S. Blügel, Phys. Rev. Lett. **86**, 4132 (2001)
9. L. Limot, J. Kröger, R. Berndt, A. Garcia-Lekue, W.A. Hofer, Phys. Rev. Lett. **94**, 126102 (2005)
10. J. de la Figuera, J.E. Prieto, C. Ocal, R. Miranda, Phys. Rev. B **47**, 13043 (1993)
11. M.Ø. Pedersen, I.A. Bönicke, E. Laegsgaard, I. Stensgaard, A. Ruban, J.K. Nørskov, F. Besenbacher, Surf. Sci. **387**, 86 (1997)

12. N.N. Negulyaev, V.S. Stepanyuk, P. Bruno, L. Diekhöner, P. Wahl, K. Kern, Phys. Rev. B **77**, 125437 (2008)
13. L. Diekhöner, M.A. Schneider, A.N. Baranov, V.S. Stepanyuk, P. Bruno, K. Kern, Phys. Rev. Lett. **90**, 236801 (2003)
14. O. Pietzsh, A. Kubetzka, M. Bode, R. Wiesendanger, Phys. Rev. Lett. **92**, 057202 (2004)
15. M.V. Rastei, B. Heinrich, L. Limot, P.A. Ignatiev, V.S. Stepanyuk, P. Bruno, J.P. Bucher, Phys. Rev. Lett. **99**, 246102 (2007)
16. B. Voigtländer, G. Meyer, Amer, M. Nabil, Phys. Rev. B **44**, 10354 (1991)
17. S. Padovani, I. Chado, F. Scheurer, J.P. Bucher, Phys. Rev. B **59**, 11887 (1999)
18. H. Bulou, J.-P. Bucher, Phys. Rev. Lett. **96**, 076102 (2006)
19. I. Chado, C. Goyhenex, H. Bulou, J.P. Bucher, Phys. Rev. B **69**, 085413 (2004)
20. M.V. Rastei, J.P. Bucher, P.A. Ignatiev, V.S. Stepanyuk, P. Bruno, Phys. Rev. B **75**, 045436 (2007)
21. K. Schouteden, E. Lijnen, E. Janssens, A. Ceulemans, L.F. Chibotaru, P. Lievens, C. Van Haesendonck, New J. Phys. **10**, 043016 (2008)
22. I.E. Tamm, Z. Phys. **76**, 849 (1932)
23. W. Shockley, Phys. Rev. **56**, 317 (1939)
24. H. Lüth, Appl. Phys. A: Mat. Sci. Proc. **8**, 1 (1975)
25. M.F. Crommie, C.P. Lutz, D.M. Eigler, Nature **363**, 524 (1993)
26. J. Li, W.-D. Schneider, R. Berndt, S. Crampin, Phys. Rev. Lett. **80**, 3332 (1998)
27. L. Niebergall, V.S. Stepanyuk, J. Berakdar, P. Bruno, Phys. Rev. Lett. **96**, 127204 (2006)
28. O. Pietzsch, S. Okatov, A. Kubetzka, M. Bode, S. Heinze, A. Lichtenstein, R. Wiesendanger, Phys. Rev. Lett. **96**, 237203 (2006)
29. K. Wildberger, V.S. Stepanyuk, P. Lang, R. Zeller, P.H. Dederichs, Phys. Rev. Lett. **75**, 509 (1995)
30. R. Zeller, P.H. Dederichs, Phys. Rev. B **52**, 8807 (1995)
31. J. Zabloudil, R. Hammerling, L. Szunyogh, P. Weinberger, *Electron Scattering in Solid Matter* (Springer Series in Solid-State Sciences, Springer-Verlag, Berlin, 2005), Vol. 147
32. O.V. Lysenko, V.S. Stepanyuk, W. Hergert, J. Kirschner, Phys. Rev. Lett. **89**, 126102 (2002)
33. F. Meier, K. von Bergmann, P. Ferriani, J. Wiebe, M. Bode, K. Hashimoto, S. Heinze, R. Wiesendanger, Phys. Rev. B **74**, 195411 (2006)
34. S.N. Okuno, T. Kishi, K. Tanaka, Phys. Rev. Lett. **88**, 066803 (2002)
35. J. Friedel, in *The Physics of Metals: Electrons*, edited by J.M. Ziman (Cambridge University Press, London, 1969), Vol. I
36. C.Q. Sun, Prog. Mat. Sci. **54**, 179 (2009)
37. V.S. Stepanyuk, D.I. Bazhanov, A.N. Baranov, W. Hergert, P.H. Dederichs, J. Kirschner, Phys. Rev. B **62**, 15398 (2000)
38. O. Mironets, H.L. Meyerheim, C. Tusche, V.S. Stepanyuk, E. Soyka, P. Zschack, H. Hong, N. Jeutter, R. Felici, J. Kirschner, Phys. Rev. Lett. **100**, 096103 (2008)
39. V. Rosato, B. Guillope, B. Legrand, Philos. Mag. A **59**, 321 (1989)
40. M. Bode, Rep. Prog. Phys. **66**, 523 (2003)
41. W. Wulfhekel, U. Schlikum, J. Kirschner, *Applied Scanning Probe Methods II: Scanning Probe Microscopy Techniques* (NanoScience and Technology, Applied Scanning Probe Methods, Springer Verlag 2006), Chap. 4
42. G. Rodary, S. Wedekind, D. Sander, J. Kirschner, Jpn J. Appl. Phys. **47**, 9013 (2008)
43. M.V. Rastei, J.P. Bucher, J. Phys.: Condens. Matter **18**, L619 (2006)
44. K. Schouteden, D.A. Muzychenko, C. Van Haesendonck, J. Nanosci. Nanotechnol. **8**, 3616 (2008)
45. B.W. Heinrich, C. Iacovita, M.V. Rastei, L. Limot, J.P. Bucher, P.A. Ignatiev, V.S. Stepanyuk, P. Bruno, Phys. Rev. B **79**, 113401 (2009)
46. A.F. Takács, F. Witt, S. Schmaus, T. Balashov, M. Bowen, E. Beaurepaire, W. Wulfhekel, Phys. Rev. B **78**, 233404 (2008)
47. F.E. Olsson, M. Persson, A.G. Borisov, J.-P. Gauyacq, J. Lagoute, S. Fölsch, Phys. Rev. Lett. **93**, 206803 (2004)
48. L. Limot, E. Pehlke, J. Kröger, R. Berndt, Phys. Rev. Lett. **94**, 036805 (2005)
49. V.S. Stepanyuk, A.N. Klavsyuk, L. Niebergall, P. Bruno, Phys. Rev. B **72**, 153407 (2005)
50. B. Lazarovits, L. Szunyogh, P. Weinberger, Phys. Rev. B **73**, 045430 (2006)
51. S. Lounis, P. Mavropoulos, P.H. Dederichs, S. Blügel, Phys. Rev. B **73**, 195421 (2006)
52. W.A. Hofer, A. Foster, A. Shluger, Rev. Mod. Phys. **75**, 1287 (2003)
53. W.A. Hofer, K. Palotás, S. Rusponi, T. Cren, H. Brune, Phys. Rev. Lett. **100**, 026806 (2008)